Earth and Planetary Science Letters 419 (2015) 32–42

Contents lists available at ScienceDirect

Earth and Planetary Science Letters

www.elsevier.com/locate/epsl

Mg and Ca isotope signatures of authigenic dolomite in siliceous deep-sea sediments

Clara L. Blättler [a,*], Nathaniel R. Miller [b], John A. Higgins [a]

[a] Princeton University, Department of Geosciences, Guyot Hall, Princeton, NJ 08544, USA
[b] The University of Texas at Austin, Department of Geological Sciences, 1 University Station C1100, Austin, TX 78712, USA

ARTICLE INFO

Article history:
Received 4 November 2014
Received in revised form 26 February 2015
Accepted 5 March 2015
Available online 19 March 2015
Editor: J. Lynch-Stieglitz

Keywords:
dolomite
authigenic carbonate
magnesium isotopes
calcium isotopes
Monterey formation

ABSTRACT

Authigenic carbonates in marine sediments frequently have carbon isotope ratios that reflect local organic carbon processing rather than the $\delta^{13}C$ of the global DIC (dissolved inorganic carbon) reservoir, but their contributions to ancient sedimentary sections are difficult to assess. In this study of authigenic dolomite from the Miocene-age Monterey Formation of offshore California, Mg and Ca isotopes are shown to vary with stratigraphic depth as a result of early diagenetic processes. The dolomite is a pre-compaction authigenic phase that occurs as beds and nodules with $\delta^{13}C$ ranging from −16 to +9‰. Light $\delta^{13}C$ values were likely acquired from the sedimentary zone of microbial sulfate reduction, while heavy $\delta^{13}C$ values were acquired from the zone of methanogenesis. Mg and Ca isotopes are roughly anti-correlated, with intervals of negative $\delta^{13}C$ associated with low $\delta^{26}Mg$ and higher $\delta^{44/40}Ca$ values. The variability is observed over a wide range of length-scales, from 10^{-2} meters within individual authigenic beds/nodules, to 10^{2} meters over the entire stratigraphic column, and can be understood as the consequence of dolomite precipitation in pore fluids where Mg supply is limited by diffusive transport. The relationship of $\delta^{26}Mg$ and $\delta^{44/40}Ca$ to the more common stable isotope measurements of $\delta^{13}C$ and $\delta^{18}O$ represents a new, diagenetically robust, geochemical fingerprint for identifying synsedimentary authigenic carbonates in the geological record.

1. Introduction

The importance of authigenic carbonates in sedimentary sequences has long been recognized (e.g. Mozley and Burns, 1993), but these precipitates have recently attracted attention as possible influences on both local and global expressions of bulk carbonate $\delta^{13}C$ values (Schrag et al., 2013). According to compiled marine pore-fluid data, they could represent a non-trivial fraction of the modern alkalinity removal flux (Sun and Turchyn, 2014), and likely constituted a much more important sink in the geological past when a more reducing and higher dissolved inorganic carbon (DIC) ocean favored precipitation on and in the seafloor (Higgins et al., 2009). The presence of authigenic carbonate is sometimes obvious, as in nodules or layers associated with organic-rich shelf sediments (e.g. Malone et al., 2002), but may also be more subtle. Changes in carbonate geochemistry have been observed on 10^{-5} m scales, affected by diagenetic phases only evident with micro-imaging techniques (Kozdon et al., 2009). Determining the presence of authigenic carbonates based on texture or trace-element composition may be particularly difficult when sedimentary components have recrystallized during burial and lithification.

Identifying authigenic phases in marine carbonates is particularly important when interpreting carbonate $\delta^{13}C$ records, which can be affected by isotopic changes in the global DIC reservoir, or by incorporation of pore fluid DIC with variable $\delta^{13}C$. The classic model of Claypool and Kaplan (1974) for pore fluid $\delta^{13}C$ attributes low $\delta^{13}C$ (−20 to −25‰) to zones of bacterial sulfate reduction (BSR), whereas high $\delta^{13}C$ (up to +20‰) reflects deeper methanogenic zones. The formation of authigenic carbonate within these metabolic zones can result in the incorporation of the pore-fluid $\delta^{13}C$, leading to a sedimentary record that may have little connection to $\delta^{13}C$ changes in the global DIC reservoir (Schrag et al., 2013). Given the potential for generating apparent $\delta^{13}C$ excursions from post-depositional processes, additional geochemical tools are needed to verify the presence of authigenic phases.

This study demonstrates the potential utility of Mg and Ca isotope analyses as geochemical tracers for authigenic carbonate formation in marine sediments. The Mg and Ca isotope systems should be useful for this application because both pore-fluid $\delta^{26}Mg$ and $\delta^{44/40}Ca$ can change with depth (Higgins and Schrag, 2010;

* Corresponding author. Tel.: +1 617 678 6211.
E-mail addresses: blattler@princeton.edu (C.L. Blättler), nrmiller@jsg.utexas.edu (N.R. Miller), jahiggin@princeton.edu (J.A. Higgins).

http://dx.doi.org/10.1016/j.epsl.2015.03.006
0012-821X/

Fantle and DePaolo, 2007) and the isotopic composition of authigenic phases may be sensitive to where in the sediment column they precipitate (see Sections 6.3 and 6.4 below). In addition, as the major cations in common authigenic carbonates (i.e. calcite and dolomite), these alkaline earth elements are also relatively robust to subsequent diagenetic alteration. Considering likely diagenetic fluids, these isotopic systems should only be affected at water/rock ratios that approach those needed to completely reset $\delta^{13}C$ values, and are thus particularly suitable for deconvolving the primary and diagenetic origins of $\delta^{13}C$ in marine carbonates. This behavior contrasts with mineralogical, crystallographic, and trace-element properties of carbonates which are more easily disturbed and therefore less reliable tracers of bulk geochemical alteration. Together, the traditional isotopic measurements of $\delta^{13}C$ and $\delta^{18}O$, paired with the newer systems of $\delta^{26}Mg$ and $\delta^{44/40}Ca$, can provide a robust picture of primary and post-depositional geochemical processes. Using analyses of Mg and Ca isotopes from the Monterey Formation, a well characterized siliceous formation containing early diagenetic dolomite (Bramlette, 1946), this study suggests that multi-isotope analyses can serve as a useful geochemical fingerprint of authigenesis and diagenesis, which may have broad utility in disentangling the local or global signals stored in the geochemistry of ancient sedimentary carbonates.

2. Background

The Monterey Formation is a siliceous, organic-rich, pelagic to hemi-pelagic sedimentary sequence of Miocene age, accessible both onshore and offshore central and southern California (Bramlette, 1946; Pisciotto and Garrison, 1981). Where it has attained sufficient burial depth, it is a significant hydrocarbon source rock (Pisciotto and Garrison, 1981), with an average of 2 to 5% but up to 23% TOC (total organic carbon), depending on lithology (Isaacs and Petersen, 1987). The dolomite of the Monterey Formation occurs as beds and nodules, possibly associated with zones of more concentrated foraminiferal carbonate (Bramlette, 1946; Friedman and Murata, 1979). Sedimentary layering thickens as it runs through nodules, indicating that the dolomite formed as an early diagenetic concretionary phase prior to sediment compaction (Bramlette, 1946). Anaerobic respiration pathways of organic carbon during sediment burial are likely to have encouraged dolomite formation by removing dolomite-inhibiting sulfate through bacterial sulfate reduction (BSR) and by increasing carbonate alkalinity in pore fluids (Baker and Kastner, 1981), though the exact mechanisms are still debated (e.g. Compton, 1988; Mazzullo, 2000; Vasconcelos et al., 1995).

Carbon isotopes in Monterey Formation dolomite cover a wide range of values that have been linked to different zones of metabolic activity during aqueous phase diagenesis (e.g. Pisciotto and Mahoney, 1981; Hennessy and Knauth, 1985; Burns and Baker, 1987). Coherent, stratigraphic trends may be a function of sedimentation rate and/or organic matter content, with higher sedimentation rates (or more organic matter) leading to rapid respiration of organic matter, a shallow transition to anaerobic oxidation pathways and depletion of sulfate, and therefore isotopically heavy carbonates (Pisciotto and Mahoney, 1981). Isotopic variation can develop stratigraphically, laterally, or even within a single nodule, based on the growth history of carbonate within different zones (Hennessy and Knauth, 1985).

The interpretation of dolomite oxygen isotopes in the Monterey Formation remains unresolved, with multiple mechanisms proposed to explain different patterns of co-variation between $\delta^{13}C$ and $\delta^{18}O$ (e.g. Hennessy and Knauth, 1985; Malone et al., 1994). The Claypool model described above predicts a negative correlation between carbon and oxygen isotopes, as higher $\delta^{13}C$ values are acquired at greater depths and temperatures. However, the observed ranges for dolomite $\delta^{18}O$ (often $>5‰$) are greater than can be explained by the oxygen isotope paleothermometer (only 1.3‰ for 100 m burial depth with a geothermal gradient from Boles et al., 2004 of 50 °C/km and the temperature calibration of Vasconcelos et al., 2005) under the shallow conditions implied by sedimentary textures. An alternative explanation for carbon and oxygen isotope trends invokes the recrystallization of dolomite during burial and the resetting of $\delta^{18}O$, or both $\delta^{13}C$ and $\delta^{18}O$, which can explain positively correlated $\delta^{13}C$ and $\delta^{18}O$ in some environments (Hennessy and Knauth, 1985; Burns and Baker, 1987; Malone et al., 1994). Clumped-isotope paleothermometry also supports deeper (hotter) recrystallization at a single locality (Loyd et al., 2012), but requires an additional mechanism to alter pore-fluid $\delta^{18}O$. With multiple possible interpretations of both $\delta^{13}C$ and $\delta^{18}O$ of dolomites, it is clear that additional geochemical constraints are needed to resolve the processes controlling these geochemical signals.

3. Materials and methods

Samples analyzed in this study are from a marine drill-core recovered at Platform Holly in the South Elwood offshore oil field, a few kilometers off the California coast in the Santa Barbara Basin (Miller, 1995). The drill site is at the crest of an anticlinal fold, and the core contains opal-CT grade silica, with very minor chert, and thermally immature oils (Orr, 1986). Dolomite occurs in discrete intervals throughout the core, and two sets of samples were collected and processed in different ways.

The first set (Figs. 1 and 2) was sampled from central portions of the dolomite intervals and treated to isolate the dolomite fraction. First, minor calcite content was preferentially dissolved using iterative treatments of 0.27 M disodium EDTA solution buffered to pH 6.3 (Videtich, 1981), and the dolomite fraction was collected by filtration. From this dolomite fraction, C and O isotopes were analyzed using traditional stable isotope techniques (Miller, 1995). The dolomite was then dissolved for Mg and Ca isotope analysis using a 0.1 M solution of buffered acetic acid–ammonium hydroxide over 3–4 h in an ultrasonicating bath, followed by centrifugation and transfer of the supernatant to a clean vial.

The second sample set was processed to permit comparison between different carbonate components within the core (Fig. 3). For this purpose, a ~3.5 m interval, including two dolomite horizons, was sampled in high resolution (every ~3 cm). The entire carbonate fraction (both calcite and dolomite) was dissolved in 0.33 M acetic acid using a volume of acid capable of only dissolving 80% of the total carbonate, to limit leaching of non-carbonate phases, and from this dissolved fraction, Mg and Ca isotopes were analyzed.

Dissolved samples were prepared for Mg and Ca isotope measurements using both traditional gravity-driven ion-exchange chemistry as well as an automated ion chromatography (IC) system. The traditional methods, which are much more time- and labor-intensive, use large volumes (>10 mL) of strong acids (2–6 N HCl) to elute cations from resin-filled columns, and for Ca separation, a second column elution step is also required to remove Sr. The procedures involve manually cleaning, loading, and collecting samples from the columns. An alternative method for ion separation uses a Dionex ICS-5000^{+} IC system coupled with a Dionex AS-AP fraction collector. This system allows for efficient, automated cation separation of both Mg and Ca. Samples are injected in 0.2% HNO_3 and passed through a Dionex CS-16 cation-exchange column using methyl-sulfonic acid (MSA) as the eluent at a flow rate of 1 mL/min. The conductivity of each sample is measured and the sample collected in the desired time window. Elution times per sample, including column washing, range from 30 to 50 min, depending on the matrix. Blank levels are equivalent for both

sample preparation systems, yielding <5 ng for both Mg and Ca, or $<1\%$ and $<0.1\%$ of the sample mass, respectively (500 ng for Mg and 5000 ng for Ca). Sample yields can be independently verified with chromatograms generated for each sample, and problematic samples can be excluded from isotopic analyses. The automated Dionex IC system yields high sample throughput with excellent reproducibility, and was used for all Mg isotope analyses in this study and a fraction of the Ca isotope analyses (see supplemental data tables). Following ion separation, samples were treated with concentrated HNO_3, then dried and re-diluted to the appropriate concentrations for mass spectrometry.

Isotopic analysis of samples was carried out on a Neptune Plus multi-collector ICP-MS (inductively coupled plasma mass spectrometer) at Princeton University. Mg isotope analyses typically require ~500 ng of Mg, diluted to 150–200 ppb in 2% HNO_3. Sample-standard-sample bracketing is used to correct for instrumental mass fractionation (Galy et al., 2001). Calcium isotope analyses require samples of ~5 µg Ca which are run as 2–4 ppm Ca solutions in 2% HNO_3. Analyses are performed with an ESI Apex-IR sample introduction system, which reduces hydride interferences significantly, but not entirely. To avoid further interferences, a medium-resolution slit is used so that the ^{42}Ca beam can be measured on the low-mass side, avoiding ArH_2^+. Sample and standard solutions are also carefully diluted to the same concentration to minimize concentration-dependent isotope effects. The beam at $m/z = 43.5$, which records the contribution of $^{87}Sr^{2+}$, is used to correct for $^{88}Sr^{2+}$ and $^{86}Sr^{2+}$ interferences, if any, on the Ca isotope beams. External precision is based on the long-term reproducibility of replicate standard analyses with a carbonate-like matrix, which are processed regularly with each batch of samples, and is 0.11‰ for $\delta^{26}Mg$ and 0.08‰ for $\delta^{44/42}Ca$ (2σ).

The accuracy of these analytical methods is confirmed by measurement of inter-laboratory standards. Mg isotope ratios are reported relative to the standard DSM-3, and Ca isotope ratios are reported relative to modern seawater. For Mg, $\delta^{26}Mg$ of the Cambridge-1 standard measured at -2.59 ± 0.06‰ agrees well with measurements of other laboratories (Galy et al., 2003). For comparison with Ca isotope data generated by TIMS, $\delta^{44/42}Ca$ values derived from ICP-MS analyses are converted to $\delta^{44/40}Ca$ relative to modern seawater using in-house seawater analyses. A difference in $\delta^{44/40}Ca$ of -1.15‰ is measured between seawater and the carbonate standard SRM-915b, which also agrees with published data (Heuser and Eisenhauer, 2008). As a check for mass-dependent variations in measured $\delta^{26}Mg$ and $\delta^{44/40}Ca$ values, all data are evaluated on a triple-isotope plot (e.g. $\delta^{25}Mg$ vs $\delta^{26}Mg$) and samples that deviate significantly from the terrestrial mass-dependent line are discarded. The slope of $\delta^{25}Mg$ vs $\delta^{26}Mg$ for the dolomite data is 0.52, and the slope for $\delta^{44/43}Ca$ vs $\delta^{44/42}Ca$ is 0.45, which are close matches to the expected mass-dependence laws. The accuracy of the Dionex IC system was evaluated by measuring the Mg and Ca isotopic composition of samples and standards processed by both the IC system and traditional gravity columns, and the same degree of accuracy and precision described above are obtained by both methods.

4. Results

Bulk dolomite $\delta^{13}C$ values throughout this section of the Monterey Formation span over 25‰, from -16.5‰ to $+9$‰ (Miller, 1995; Miller and Leybourne, 2010), and correlate in particular intervals with $\delta^{26}Mg$, $\delta^{44/40}Ca$, and $\delta^{18}O$ (Fig. 1, and supplemental material). Stratigraphic units can be defined based on distinct geochemical behavior: unit I (1341.1–1295.4 m; 4400–4250 ft), unit II (1295.4–1173.5 m; 4250–3850 ft), unit III (1173.5–1066.8 m; 3850–3500 ft), and unit IV (1066.8–1036.6 m; 3500–3400 ft). In unit I, $\delta^{13}C$ values drop from $+9$ to $+1$‰, with high $\delta^{26}Mg$ (-1.0‰), low $\delta^{44/40}Ca$ (-0.9‰), and a 4‰ range in $\delta^{18}O$. Unit II contains the minimum $\delta^{13}C$ values in this section, with $\delta^{13}C$ ranging from -5 to -16.5‰, while Mg isotopes drop to around -2.0‰ and Ca isotope ratios remain low around -0.8‰. Oxygen isotopes remain within the same range as in unit I, and show a slight anti-correlation with $\delta^{13}C$.

Unit III shows the most striking geochemical correlations in this section. A strong linear relationship between $\delta^{13}C$ and $\delta^{18}O$ ($R^2 = 0.83$) exists during this interval (see Fig. 2). Carbon isotope ratios are between -3.5 and -11.0‰; oxygen isotopes vary between $+1.0$ and $+4.5$‰. The maximum in $\delta^{18}O$ is associated with the minimum values for $\delta^{26}Mg$ (-2.6 to -2.8‰) and maximum values for $\delta^{44/40}Ca$ (-0.5 to -0.3‰). These isotopic excursions have slightly different shapes, but are all expressed during the same depth interval. Unit IV signals the end of these excursions with a return to the geochemical characteristics of unit I, with distinctly positive $\delta^{13}C$ ($+1.5$ to $+8.0$‰) and recovery of high $\delta^{26}Mg$, low $\delta^{44/40}Ca$, and low $\delta^{18}O$.

These four units occupy distinctly different areas on cross-plots of oxygen vs carbon isotopes as well as calcium vs magnesium isotopes (Fig. 2). Units I and IV have overlapping $\delta^{13}C$ values, as do units II and III, but are separated into different populations by their $\delta^{18}O$ values. Units I and IV also overlap in Ca–Mg isotope space, whereas units II and III have distinct populations with respect to these two isotope systems. The highest $\delta^{44/40}Ca$ values are only expressed within unit III, with lower values in units I, II, and IV, whereas $\delta^{26}Mg$ values are distinct for both units II and III. Magnesium isotopes are loosely correlated with C isotopes ($R^2 = 0.54$) and anti-correlated with O isotopes ($R^2 = 0.65$), with much weaker associations between Ca and C ($R^2 = 0.18$) and Ca and O ($R^2 = 0.27$).

Mg and Ca results from the high-resolution section (3829–3817 ft; 1167–1163 m) show distinct patterns based on lithology and characterize the compositional variation that is present within the core (Fig. 3, and supplemental material). Across the dolomite intervals, $\delta^{26}Mg$ and $\delta^{44/40}Ca$ are fairly uniform (-2.3‰ and -1.0‰, respectively) and match the values measured in bulk samples from that interval of unit III. Outside of the dolomite intervals, where the carbonate content reflects Fe- and Mn-rich calcite, the isotope ratios are much more variable. Magnesium isotopes vary from -2.7‰ to a maximum of -1.3‰. Calcium isotopes also vary erratically between -1.2 and -0.6‰ outside of the dolomite horizons.

The compelling stratigraphic variability in Mg and Ca isotopes, and their co-variation with carbonate C and O isotopes, begs the question: does $\delta^{26}Mg$ and $\delta^{44/40}Ca$ variability reflect changes in isotopic fractionation or the incorporation of pore-fluid Mg and Ca whose isotopic composition changes with depth? To address this question, the results are compared with a numerical model of dolomite precipitation within a static sediment column, which quantitatively explores how variations in sedimentation rate and the depth/rate of dolomite precipitation can produce the observed trends in $\delta^{26}Mg$ and $\delta^{44/40}Ca$ and their co-variation with $\delta^{13}C$ and $\delta^{18}O$.

5. Numerical pore-fluid model

The objective of the model is to determine if changes in the depth of dolomite formation can produce the observed range and co-variation between the different isotopic systems ($\delta^{26}Mg$, $\delta^{44/40}Ca$, and $\delta^{13}C$). The critical assumptions of the model are: 1) dolomite precipitation occurs at a particular depth horizon within the sediment column, and 2) pore-fluid profiles of $\delta^{26}Mg$, $\delta^{44/40}Ca$, and $\delta^{13}C$ are controlled by dolomitization, recrystallization, and pathways of organic carbon respiration, respectively. Although the model does not include every process that may have

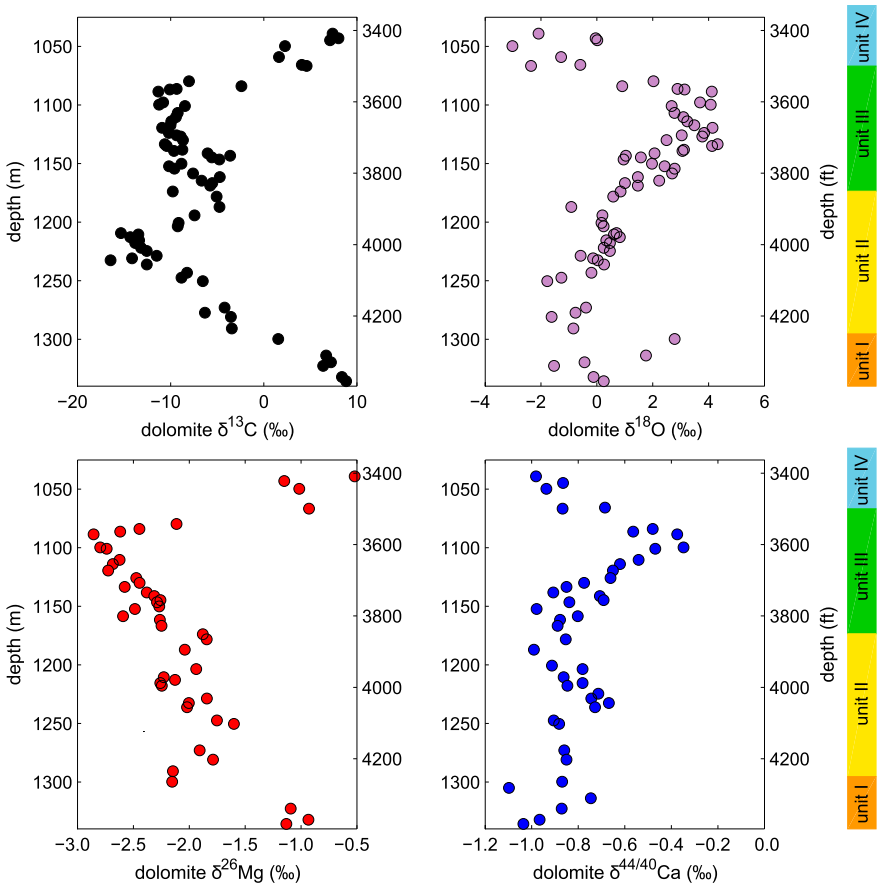

Fig. 1. Isotopic data for bulk dolomite samples from the Monterey Formation, plotted against stratigraphic depth. Delta values are reported relative to VPDB (C and O), DSM-3 (Mg), and modern seawater (Ca). The dataset includes 45 analyses each of Mg isotopes and Ca isotopes.

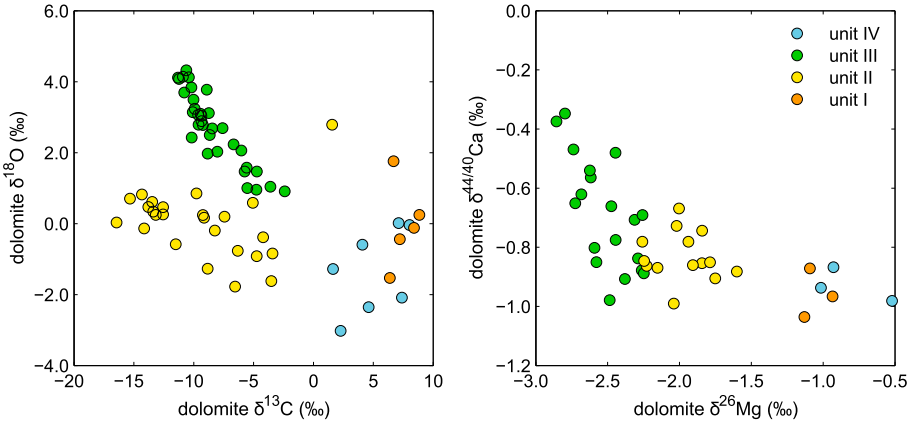

Fig. 2. Isotopic crossplots of δ^{18}O vs δ^{13}C and $\delta^{44/40}$Ca vs δ^{26}Mg for bulk dolomite samples. The four units are defined by depth and are in stratigraphic order, as described in the text (Section 4) and Fig. 1.

been occurring under the depositional conditions of the Monterey Formation, it is intended to capture the processes which likely dominate the subsurface budgets of Mg and Ca.

The chemistry of pore fluids and authigenic dolomite was modeled using a simplification of the generic diffusion–advection–reaction equation (adapted from Boudreau, 1997):

$$\frac{\partial \phi C_f}{\partial t} = \frac{\partial D\phi}{\partial z}\left(\frac{\partial C_f}{\partial z}\right) - \frac{\partial \phi v C_f}{\partial z} + \sum_i R_i$$

where ϕ is porosity, C_f is concentration in pore fluids, D is diffusivity, v is advection, R_i are reaction terms, and depth (z) is positive downwards. Based on shallow depths of dolomite formation (see Section 6.2), porosity is assumed to be constant, which fits observations from borderland basins with a similar depositional environment to the Monterey Formation (e.g. Yeats and Haq, 1981). With negligible compaction occurring at these depths, advection due to compaction is assumed to be zero and all other sources of fluid advection are neglected. Diffusivities are calculated after Boudreau (1997) and are essentially constant over the depth domain. Under these conditions and assumptions, the equation takes the form:

$$\frac{\partial C_f}{\partial t} = D\frac{\partial^2 C_f}{\partial z^2} + \sum_i R_i.$$

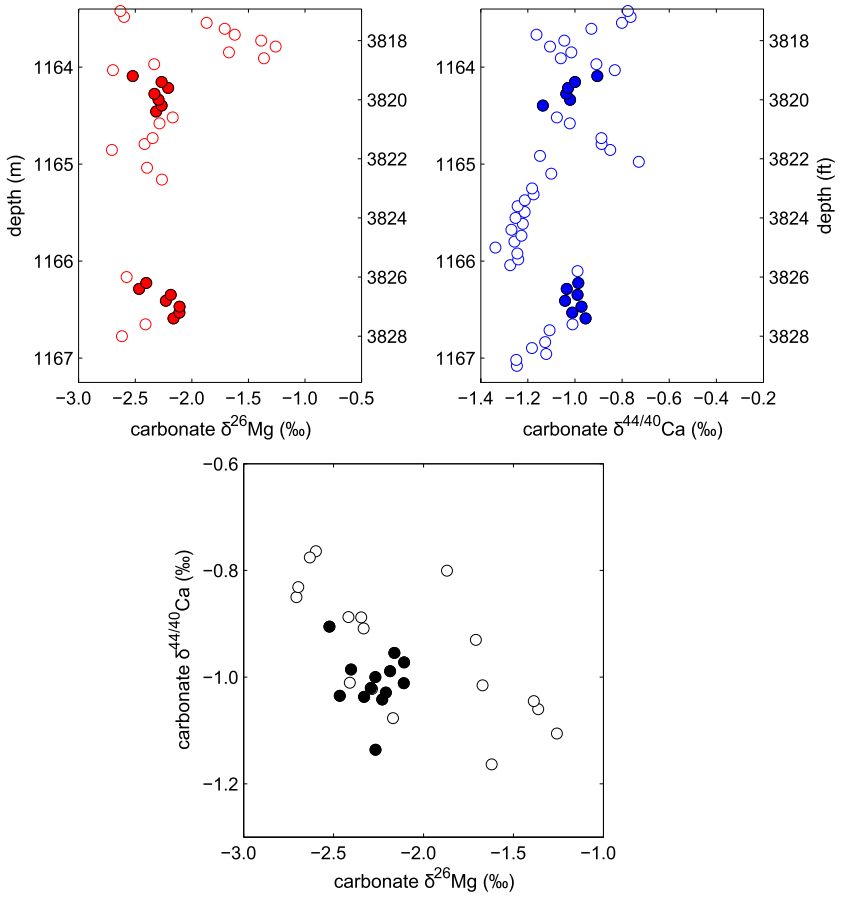

Fig. 3. Isotopic data for carbonates from a high-resolution section at the boundary between units III and IV, plotted against stratigraphic depth. Filled symbols are dolomite horizons, and open symbols are other sedimentary carbonate phases. The $\delta^{44/40}$Ca vs δ^{26}Mg crossplot includes all samples for which both Mg isotopes (35 samples analyzed) and Ca isotopes (54 samples analyzed) were measured.

The reaction terms (R_i) include calcite dissolution and precipitation, as well as authigenic dolomite growth. Clay desorption/adsorption reactions are omitted, as they are a minor component of the Monterey Formation. Calcite dissolution/precipitation reactions are explicitly incorporated because they act as the dominant control on pore-fluid Ca isotopes (Fantle and DePaolo, 2007) and dolomite horizons are often associated with foraminifera-rich beds (Bramlette, 1946; Friedman and Murata, 1979). Calcite reaction terms are defined as $f_c R_d M(C_s - nC_f)$, following the formulation of Turchyn and DePaolo (2011), where f_c is the carbonate fraction, R_d is dissolution rate (in yr^{-1}), M is the mass ratio of solid to fluid (a function of solid and fluid densities and porosity), n is the ratio of precipitation rate (R_p) to dissolution rate (R_d), and C_s and C_f are concentrations in the solid and fluid, respectively. This formulation allows for net carbonate precipitation or dissolution within the system. Dolomite growth is represented as $R_{dol} M C_s$, where R_{dol} is the rate of dolomitization.

The three rates, R_d, R_p, and R_{dol}, follow prescribed functional forms based on assumptions about the reactions, and are the primary tunable parameters in the model (see supplemental material fur further details). The rates for calcite recrystallization are set as exponentials following the assumption that rates decrease with depth (Richter and DePaolo, 1987). Given the poor understanding of dolomite formation kinetics, especially within the discontinuous nodules and horizons of the Monterey Formation, dolomitization is modeled over a limited depth interval with a subsurface maximum, a 'pulse', independent of pore-fluid Ca or Mg concentrations. This formulation produces a discrete dolomite horizon that grows within the sediment pore spaces over a given time interval, matching the observed distribution of dolomite in the sampled core.

Each modeled isotope of Mg and Ca is governed by a separate equation, related by fractionation factors estimated from published work (see supplemental material). Fractionation associated with diffusion is assumed to be negligible (Boudreau, 1997; Richter et al., 2006). Mg isotope fractionation during dolomite formation follows $\alpha_{dol}^{\mathrm{Mg}} = 0.998$ (Higgins and Schrag, 2010), while recrystallization follows the equilibrium fractionation $\alpha_d^{\mathrm{Ca}} = \alpha_p^{\mathrm{Ca}} = 1$ (Fantle and DePaolo, 2007; Jacobson and Holmden, 2008). With uncertainty in the Ca isotope fractionation for dolomite, a range of values from $\alpha_{dol}^{\mathrm{Ca}} = 1$ to 0.9996 are used. The calcite fraction of the initial sediment column reflects $\alpha_{cc} = 0.9987$ relative to seawater (Fantle and DePaolo, 2007).

This model construction is designed to replicate the effects of a dolomite horizon nucleating and growing within a sediment column, before a possible hiatus in dolomite formation and renucleation at another location in the sediment. The results illustrate the range of possible isotopic signals that can be generated with these processes, and that might be present at different times within a more realistic scenario where sediment accumulates over time. Carbon speciation, carbon isotopes, and alkalinity are not calculated or specified in the model, but a generic δ^{13}C depth curve is included with model output to emphasize the characteristic δ^{13}C values that may be incorporated from pore-fluid DIC during dolomite formation.

6. Discussion

Based on classic sedimentological analyses of Monterey Formation dolomites (Bramlette, 1946) and records of deep ocean δ^{13}C

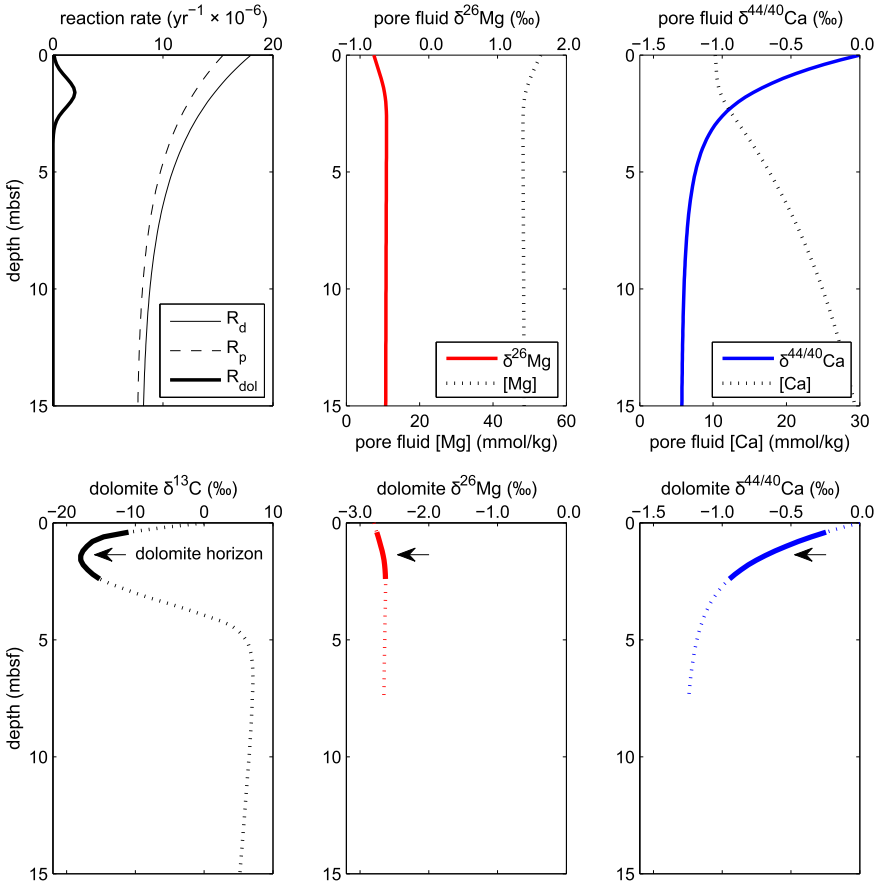

Fig. 4. Model results for a simulated dolomite growth event, where dolomitization at 1.6 m depth generates 22 weight % dolomite over 10^5 yr with isotopic characteristics similar to units II and III. Pore fluid profiles and dolomite composition are plotted against burial depth within a static sedimentary column, with arrows marking peak dolomite intervals.

during the Miocene (Cramer et al., 2009), the wide range in δ^{13}C of these dolomite nodules is best interpreted as the result of early diagenetic processes in the sediment column, rather than primary oceanographic signals of the global carbon cycle. The observed correlations between C, O, Mg, and Ca isotopes in units II and III are striking and suggest a mechanistic connection among these geochemical properties. However, there are also intervals where the correlations are much weaker or non-existent, suggesting that the relationships between these isotopic systems are nonlinear. The following sections explore the hypothesis that dolomite δ^{13}C, δ^{18}O, δ^{26}Mg, and $\delta^{44/40}$Ca are primary signals in the Monterey Formation, related through pore-fluid geochemistry and/or the kinetics of dolomite formation. Section 6.5 then discusses how δ^{26}Mg and $\delta^{44/40}$Ca patterns can act as geochemical fingerprints for authigenic carbonates in similar environments with non-unique interpretations for δ^{13}C.

6.1. Carbon isotopes

Large variation in δ^{13}C can result from authigenic dolomite forming within different metabolic reaction zones in the sediment column and inheriting the characteristic pore-fluid δ^{13}C of those zones (Claypool and Kaplan, 1974). An increase in alkalinity that promotes carbonate precipitation occurs in the zones of bacterial sulfate reduction (BSR) and anaerobic methane oxidation (AMO), which establishes a region of possible dolomite formation where pore-fluid δ^{13}C first decreases and then eventually increases with depth (e.g. Fig. 4). However, the relationship between dolomite formation and alkalinity production in the sediment column is not simple, as variability in dolomite δ^{13}C requires that the zone of most abundant dolomite formation migrates relative to these metabolic zones. One possibility for driving changes in the depth of dolomite formation is a change in sedimentation rate and the depth of sulfate diffusion into the sediment column. For example, higher sedimentation rates can lead to more intense organic matter respiration and sulfate depletion, and with limited diffusion of oxidants from overlying seawater, the transition to anaerobic respiration pathways occurs quicker (shallower) (Pisciotto and Mahoney, 1981). A shallow transition to anaerobic respiration pathways would predict dolomite formation in the methanogenic zone with high δ^{13}C; under low sedimentation rates, the aerobic and BSR zones extend to greater depths and dolomite can form in the zone of BSR/AMO with negative δ^{13}C, provided there are organic substrates for dolomite nucleation and sufficient reactants. Within this framework, the interval from unit I to II in this section of the Monterey Formation would reflect a decrease in sedimentation rate, while the transition from unit III to IV would reflect an increase in sedimentation rate. This interpretation is consistent with observations and models from several localities of authigenic dolomite formation in organic-rich sediments (Baker and Burns, 1985; Compton and Siever, 1986), as well as with trace metal (Fe, Mn, REE) behavior observed in the dolomites in this study (Miller and Leybourne, 2003, 2010) and in other sections of the Monterey Formation (Burns and Baker, 1987).

6.2. Oxygen isotopes

O isotope ratios of Monterey Formation dolomites show a range of 7‰ that is both stratigraphically coherent and co-varies with δ^{26}Mg, δ^{13}C, and $\delta^{44/40}$Ca. This variability is difficult to explain by

conventional means. One possible mechanism for acquiring light $\delta^{18}O$ in dolomites, despite the shallow depths required for nodule growth, is for concretions initially composed of protodolomite to recrystallize to more ordered dolomite at depth, allowing $\delta^{18}O$ to equilibrate at a higher temperature (Hennessy and Knauth, 1985; Burns and Baker, 1987; Malone et al., 1994). Given the high ratio of oxygen in pore fluids relative to dolomite (much greater than the highly rock-buffered C, Mg, or Ca), it is theoretically possible for oxygen to be the only isotopic system reset during such a reaction. However, the good correlation between Mg and O isotopes and the strong inverse correlation between C and O isotopes during unit III (Fig. 2) implies a primary depositional relationship.

If stratigraphic variability in dolomite $\delta^{18}O$ is an early diagenetic signal, there are three possible drivers: changes in temperature, changes in pore-fluid $\delta^{18}O$, or kinetic isotope effects. The temperatures calculated from the dolomite–water equilibrium calibration of $1000 \cdot \ln(\alpha) = 2.73 \cdot 10^6 \cdot T^{-2} + 0.26$ (Vasconcelos et al., 2005), using bottom water $\delta^{18}O$ of -1‰ (VSMOW), range from 0 to 33 °C, corresponding to burial depths up to 660 m for the geothermal gradient (50 °C per km) measured at Platform Holly (Boles et al., 2004), where these samples were drilled. Such great depths cannot reflect the locations of dolomite precipitation in the Monterey Formation, which are constrained to be at pre-compaction depths and within the range of diffusive supply of Mg from seawater, on the order of 10^0–10^1 m (Baker and Burns, 1985; Burns and Baker, 1987; Compton and Siever, 1986). Even allowing for higher geothermal gradients and a possible 0.7‰ increase in bottom water $\delta^{18}O$ during the Miocene (Flower and Kennett, 1994), only ~1‰ of the observed change can be explained by these means.

Isotopically light pore fluids can be generated from exchange between water and volcanic material, precipitation of ^{18}O-enriched carbonates, or the influence of meteoric water (Lawrence et al., 1975; Mozley and Burns, 1993), but none of these processes are likely to have been capable of driving such large $\delta^{18}O$ variability in shallow pore fluids during deposition of the Monterey Formation. Organic matter respiration by sulfate reduction, generating ^{13}C-depleted bicarbonate, is another possible source of light $\delta^{18}O$ in authigenic carbonate (Sass et al., 1991), with the added advantage of providing a direct link to low $\delta^{13}C$ values. However, this mechanism would require extremely high organic carbon contents, at least locally, to generate such light $\delta^{18}O$ values. Gas hydrate formation could also affect the $\delta^{18}O$ of pore fluids during the formation of ^{18}O-enriched clathrates (Hesse and Harrison, 1981), but relatively warm bottom-water temperatures during the Miocene may not have permitted this process. Given large uncertainties in the growth rates for these authigenic dolomites and a complete lack of knowledge of the rate dependence (if any) of $\delta^{18}O$ during dolomite precipitation (e.g. DePaolo, 2011), kinetic isotope effects also cannot be ruled out (but see further discussion on kinetics in Section 6.4).

6.3. Magnesium isotopes

In sediments where dolomite is actively precipitating in the subsurface, the Mg isotopic composition of the pore fluid is distilled to heavier values by the removal of Mg to dolomite that is depleted in ^{26}Mg relative to the pore fluid by 2.0 to 2.7‰ (Higgins and Schrag, 2010). This behavior is expected in sedimentary environments where Mg is consumed (i.e. pore-fluid Mg concentrations decrease with depth) by carbonate formation and transport is limited by diffusion. The opposite trend, a decrease in pore-fluid $\delta^{26}Mg$ with depth, is possible in sites with net carbonate dissolution, driven by low $\delta^{26}Mg$ values for inorganic and biogenic calcium carbonates (e.g. Pogge von Strandmann, 2008; Wombacher et al., 2011), or with authigenic clay formation, because Mg-clays preferentially incorporate ^{26}Mg (Higgins and Schrag, 2010; Wimpenny et al., 2014). Neither of these processes (net carbonate dissolution or clay formation) are likely to have controlled pore-fluid profiles during deposition of the Monterey Formation, due to the large demands placed on the pore-fluid Mg budget from dolomite precipitation.

In an environment where pore-fluid $\delta^{26}Mg$ increases with depth, the Monterey Formation dolomite $\delta^{26}Mg$ data can be explained by carbonate formation at different depths within the sedimentary column, consistent with the C and O isotopic data. The minimum in $\delta^{26}Mg$ in unit III correlates with light $\delta^{13}C$ from the zone of BSR, which is interpreted to be shallower relative to unit IV and driven by low sedimentation rates. The low $\delta^{26}Mg$ values in this interval are offset from modern seawater by -2.0‰, which is within the range of the estimated fractionation factor for dolomite formation of -2.0 to -2.7‰ (Higgins and Schrag, 2010; Fantle and Higgins, 2014). This agreement suggests that these samples were formed close to the sediment–water interface, where pore-fluid $\delta^{26}Mg$ was very similar (within 0.7‰) to that of seawater. Values in this range can be generated by the numerical model described above (Section 5) given a shallow dolomitization horizon and relatively low R_{dol} (Fig. 4). Maximum $\delta^{26}Mg$ values, on the other hand, suggest that dolomite was precipitated from pore fluids enriched in ^{26}Mg by around 2.0‰ over seawater. This degree of enrichment implies the minimum removal of 61% of Mg from the pore fluids, given a -2.0‰ fractionation in a closed-system model. A greater percentage of Mg must be removed in the partially open system which is required to explain the mass of dolomite that precipitated. Model results indicate that such high $\delta^{26}Mg$ values are possible for bulk dolomite samples, even considering the integrated nature of the incorporated $\delta^{26}Mg$ signal, when forced by strong subsurface dolomitization (Fig. 5).

The volatility of $\delta^{26}Mg$ values in the high-resolution interval (Fig. 3), with values up to -1.3‰ outside of the dolomitic intervals, suggests the possible incorporation of Mg into additional authigenic minerals at greater depths, where pore-fluid $\delta^{26}Mg$ was higher than seawater $\delta^{26}Mg$. Both low and high $\delta^{26}Mg$ values are present, with the majority of the data at or near the bulk $\delta^{26}Mg$ value. This behavior is consistent with isotopic distillation of pore-fluid Mg through precipitation of authigenic dolomite, rather than kinetic isotope effects, as these precipitates are unlikely to have formed at the same rate or range of rates as the more massive dolomite beds and nodules. The shared range with bulk dolomite values suggests that these phases represent micro-scale dolomite or calcite which precipitated authigenically at different stages of burial. As minor sedimentary components of Mg, however, these phases would not exert a strong influence on pore-fluid Mg isotope composition, which is controlled by the precipitation of massive dolomite horizons.

6.4. Calcium isotopes

Ca isotopes of pore fluids have been shown to decrease with depth as sedimentary calcite recrystallizes and equilibrium is reached between sedimentary carbonate and pore-fluid Ca (Fantle and DePaolo, 2007; Turchyn and DePaolo, 2011). The equilibrium fractionation between calcite and water, observed in deep sea pore fluids (Fantle and DePaolo, 2007) and a long-lived carbonate aquifer (Jacobson and Holmden, 2008), appears to be close to 0‰, while bulk pelagic sediment expresses a calcium isotope fractionation of -1.3‰ relative to seawater (Fantle and DePaolo, 2007). Sedimentary composition appears to have a large effect on the rate of recrystallization and therefore the depth scale over which isotopic equilibrium (when sediment and pore-fluid $\delta^{44/40}Ca$ are equal) is achieved. Equilibrium occurs over < 80 m (possibly much less than 80 m) for deep sea carbonate ooze at ODP site 807A

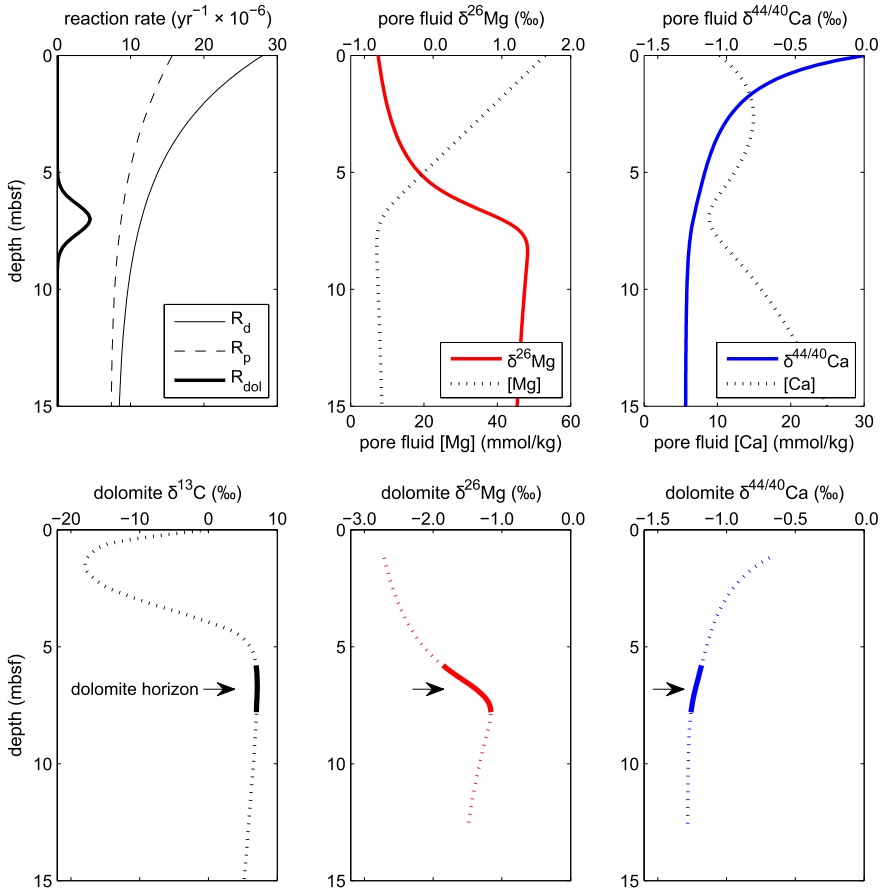

Fig. 5. Model results for a simulated dolomite growth event, where massive dolomitization at 7 m depth generates 50 weight % dolomite over 10^5 yr with isotopic characteristics similar to units I and IV. Pore fluid profiles and dolomite composition are plotted against burial depth within a static sedimentary column, with arrows marking peak dolomite intervals.

(Fantle and DePaolo, 2007), yet >500 m for clay- and organic-rich sediments at ODP sites 984 and 1082 (Turchyn and DePaolo, 2011), because of lower carbonate abundance as well as lower apparent reactivity of carbonate at sites 984 and 1082.

In the Monterey Formation, the sedimentary calcite component, mostly in the form of disseminated foraminifera and calcareous nannoplankton, averages 9.2% within the predominantly siliceous facies (Bramlette, 1946). Even with only a few weight percent, sedimentary calcite represents a much larger reservoir of Ca than pore fluids, and recrystallization reactions will lead to a decrease in pore-fluid $\delta^{44/40}$Ca with depth, from the seawater value (0‰) to the bulk sediment $\delta^{44/40}$Ca value. Assuming a constant fractionation during dolomite precipitation in the Monterey Formation, $\delta^{44/40}$Ca variability can be driven by changing the depth of dolomite formation, in a similar manner to the other isotopic systems explored in this study. Positive $\delta^{44/40}$Ca excursions, as in unit III, reflect a shallower zone of dolomite formation and incorporation of more seawater-like $\delta^{44/40}$Ca values, while intervals of lower $\delta^{44/40}$Ca reflect dolomite growth where pore-fluid Ca and sedimentary calcite are closer to isotopic equilibrium. These predictions are consistent with model results where the range of values observed in the Monterey Formation can be achieved by tuning recrystallization and dolomitization rates (Figs. 4 and 5). Maximum Ca isotope ratios occur where δ^{26}Mg values suggest that dolomite formed very close to the sediment–water interface, constraining the Ca isotope fractionation for dolomite growth to be $\leq$0.4‰.

For dolomite formation to inherit $\delta^{44/40}$Ca variability in the Monterey Formation, the approach towards Ca isotopic equilibrium must occur over the depths where dolomite is precipitating. In fact, the depth scale for $\delta^{44/40}$Ca depletion in pore fluids must be even smaller than that for pore-fluid δ^{26}Mg enrichment, based on the observation that $\delta^{44/40}$Ca undergoes a more abrupt transition toward the seawater endmember at the upper range of observed $\delta^{44/40}$Ca values (Fig. 2). Such a rapid decrease towards isotopic equilibrium between pore fluids and sediment seems in conflict with data showing a very long length-scale for equilibrium in clay- and organic-rich sediments (Turchyn and DePaolo, 2011). However, model results indicate that excess dissolution of sedimentary calcite is necessary to generate massive authigenic dolomite with high δ^{26}Mg, as the supply of Ca becomes limiting without a local sedimentary source. Consideration of pore-fluid concentration profiles led to a similar conclusion by Baker and Burns (1985). Net calcite dissolution leads to pore-fluid $\delta^{44/40}$Ca rapidly transitioning to the sedimentary calcite value. This mechanism is consistent with the observation that dolomite horizons are often associated with foraminifera-rich intervals in the Monterey Formation (Bramlette, 1946). The apparent sensitivity of $\delta^{44/40}$Ca to depth in these authigenic dolomites can therefore be linked to the existence of massive authigenic dolomites and the Ca supply required for their formation.

Kinetic isotope effects are also generally important for calcium isotope fractionation in carbonate minerals, and could provide an alternative explanation for the $\delta^{44/40}$Ca variability in authigenic dolomites. Kinetic isotope effects associated with dolomite formation have not yet been clearly determined, but a wide variety of isotopic behavior has been observed in dolomites, including both enrichment (Böhm et al., 2011) and depletion (Holmden, 2009) relative to surrounding limestones. A large range of dolomite $\delta^{44/40}$Ca values has been measured, including very heavy values close to that of seawater (−0.16‰, Komiya et al., 2008), inter-

mediate values (−0.46‰to −1.10‰, Tipper et al., 2008; Jacobson and Holmden, 2008; Fantle and Higgins, 2014), and values significantly lighter than average carbonates and the bulk silicate earth (−1.66‰, Holmden, 2009). By analogy with calcite (DePaolo, 2011), the equilibrium fractionation for dolomite is usually assumed to be close to 0‰ (Holmden, 2009), but the fractionation in various geological settings may be non-zero. At present, the kinetic isotope effects associated with dolomite formation are too unconstrained to determine how kinetics might respond to changing depositional conditions and if they are a viable alternative explanation to changing pore-fluid $\delta^{44/40}$Ca. However, laboratory experiments which show a rate dependence for calcite $\delta^{44/40}$Ca also show a strong correlation with Sr contents, and although it is uncertain whether this behavior extends to other carbonate minerals, $\delta^{44/40}$Ca values and Sr contents are not correlated in the Monterey dolomites (see supplemental material).

The high-resolution Ca isotope data provides additional support for the role of changing pore-fluid $\delta^{44/40}$Ca in driving dolomite $\delta^{44/40}$Ca. This dataset sampled bulk carbonate rather than just the dolomite fraction, so it provides a measure of the background sedimentary Ca. In agreement with other studies, the pelagic calcite component, present in the lower half of the high-resolution interval, has fairly homogeneous $\delta^{44/40}$Ca between −1.1 and −1.3‰ (Fig. 3). The dolomite intervals are distinct, showing the influence of heavier Ca isotopes from seawater. Trace calcite (<1 wt%) in the upper half of the interval has quite variable $\delta^{44/40}$Ca with a negative correlation with δ^{26}Mg. This behavior is consistent with these minor authigenic phases recording changes in the $\delta^{44/40}$Ca and δ^{26}Mg of pore fluid during sediment burial.

6.5. Applications

The coherent geochemical signals of dolomite nodules in the Monterey Formation suggest that these isotopic patterns could be used to identify authigenic carbonate in other localities, authigenic organic-associated dolomites in the geological record, and more generally, to signify the importance of local vs global processes in determining the chemistry of bulk carbonate samples. In particular, anti-correlated Mg and Ca isotopes (Fig. 2b) signify the opposing directions of pore-fluid δ^{26}Mg and $\delta^{44/40}$Ca evolution in the shallow sedimentary depths where early diagenesis occurs. Universal linear correlations between these isotopic systems should not be expected, though (favoring instead hyperbolic relationships and/or different slopes), as each isotopic system responds to different and somewhat independent forcing mechanisms. Carbon isotope patterns are largely due to metabolic reactions, whereas Mg isotopes respond to dolomite formation and Ca isotopes are influenced by carbonate recrystallization or kinetics. The overall direction of isotopic co-variation, however, is characteristic of early diagenetic processes and can lead to the recognition that bulk geochemical alteration has occurred.

Given the different residence times of these elements in the global ocean (C: 100 kyr; Ca: 1 Ma; Mg: 10 Myr), coherent stratigraphic variation with such multi-isotope analysis argues against variations in the isotopic composition of the global ocean. The co-variation of C, Mg, and Ca instead must originate from local processes. In the case of the Monterey Formation, these processes are related to depth changes in the chemical and isotopic composition of the pore fluid, which for Mg, Ca, and C is controlled by dolomitization, recrystallization, and organic matter cycling, respectively. As each of these elemental/isotopic systems are driven by a different set of related, but independent processes, different environments will express isotopic co-variation between these systems in different ways. In organic-rich settings where the transition to anaerobic metabolic pathways occurs quickly, large negative and positive δ^{13}C contributions from authigenic carbonates are possible. In organic-poor settings, the δ^{13}C effects may be limited, but δ^{26}Mg and $\delta^{44/40}$Ca signals may clearly indicate the presence of an authigenic phase or local diagenetic effects. At the very least, Mg and Ca isotope patterns that resemble those in the Monterey Formation suggest that bulk geochemical changes have occurred, with high potential for altering both δ^{13}C and δ^{18}O. As the major cations in dolomite, Mg and Ca isotopes are relatively resistant to later diagenesis, and thus represent powerful tools for assessing the geochemical fidelity of carbonate minerals.

Finally, comparison of the Mg isotope ratios of dolomites from the Monterey Formation with those from the Marion Plateau, ODP site 1196A (Fantle and Higgins, 2014), suggests that Mg isotope fractionation in these two very different environments is surprisingly similar. Dolomites from the Marion Plateau are interpreted to have formed in a system where Mg was supplied by advection and rates of dolomitization were comparatively slow, i.e. the system is relatively open for Mg. As a result, δ^{26}Mg values are homogeneous and offset from seawater by ~2‰ (−2.68 ± 0.07‰). These values are almost indistinguishable from the lowest δ^{26}Mg values from the Monterey Formation, dolomites that are interpreted here as forming near the sediment–water interface where conditions are most similar to the dolomites from the Marion Plateau, i.e. open with respect to the supply of Mg. The observation that Mg isotope fractionation during open-system dolomitization is similar in these two very different environments suggests that the Mg isotopic composition of some dolomites may prove to be a reliable archive of the Mg isotopic composition of seawater.

7. Conclusion

A multi-isotopic study of dolomite nodules in the Monterey Formation reveals strong, stratigraphically coherent signals in δ^{13}C, δ^{18}O, δ^{26}Mg, and $\delta^{44/40}$Ca, which can be related to early diagenetic processes in sedimentary pore fluids. Carbon isotopes vary through the zones of bacterial sulfate reduction to methanogenesis, and authigenic dolomite forming at these depths inherits this large variability. Oxygen and calcium isotope ratios of pore fluids likely decrease with depth, and magnesium isotope ratios increase with depth, driven by dolomitization and recrystallization reactions. The stratigraphic profiles of these isotopic systems are all consistent with dolomite formation occurring in a deeper zone in unit I, to a shallower zone in units II and III, and back to greater depths in unit IV. The anti-correlation of Mg and Ca isotopes is proposed as a geochemical fingerprint for this style of early diagenesis and a marker for bulk geochemical alteration for carbon and oxygen isotopes.

Acknowledgements

The authors acknowledge funding from the Agouron Institute (grant no. AI-F-GB25.13.2), Princeton University, and the CIFAR (Canadian Institute for Advanced Research) Global Scholars Program, and express thanks to Elizabeth Lundstrom, Doug Williams, and Scott Carpenter for laboratory assistance, as well as three anonymous reviewers for helpful comments.

Appendix A. Supplementary material

Supplementary material related to this article can be found online at http://dx.doi.org/10.1016/j.epsl.2015.03.006.

References

Baker, P.A., Burns, S.J., 1985. Occurrence and formation of dolomite in organic-rich continental margin sediments. Am. Assoc. Pet. Geol. Bull. 69, 1917–1930.

Baker, P.A., Kastner, M., 1981. Constraints on the formation of sedimentary dolomite. Science 213, 214–216. http://dx.doi.org/10.1126/science.213.4504.214.

Böhm, F., Eisenhauer, A., Fietzke, J., Rausch, S., Klügel, A., Bach, W., 2011. Calcium isotope fractionation during dolomite formation. In: Goldschmidt Conference Abstracts, Mineralogical Magazine, p. 544.

Boles, J.R., Eichhubl, P., Garven, G., Chen, J., 2004. Evolution of a hydrocarbon migration pathway along basin-bounding faults: evidence from fault cement. Am. Assoc. Pet. Geol. Bull. 88, 947–970.

Boudreau, B.P., 1997. Diagenetic Models and Their Implementation; Modelling Transport and Reactions in Aquatic Sediments. Springer, Berlin.

Bramlette, M.N., 1946. The Monterey Formation of California and the Origin of Its Siliceous Rocks. Geological Survey Professional Paper, vol. 212. US Government Printing Office.

Burns, S.J., Baker, P.A., 1987. A geochemical study of dolomite in the Monterey Formation, California. J. Sediment. Petrol. 57, 128–139. http://dx.doi.org/10.1306/212F8AC6-2B24-11D7-8648000102C1865D.

Claypool, G.E., Kaplan, I.R., 1974. The origin and distribution of methane in marine sediments. In: Kaplan, I.R. (Ed.), Natural Gases in Marine Sediments. In: Marine Science, vol. 3. Springer US, pp. 99–139.

Compton, J.S., 1988. Degree of supersaturation and precipitation of organogenic dolomite. Geology 16, 318–321. http://dx.doi.org/10.1130/0091-7613(1988)016<0318:DOSAPO>2.3.CO;2.

Compton, J.S., Siever, R., 1986. Diffusion and mass balance of Mg during early dolomite formation, Monterey Formation. Geochim. Cosmochim. Acta 50, 125–135. http://dx.doi.org/10.1016/0016-7037(86)90057-8.

Cramer, B.S., Toggweiler, J.R., Wright, J.D., Katz, M.E., Miller, K.G., 2009. Ocean overturning since the Late Cretaceous: inferences from a new benthic foraminiferal isotope compilation. Paleoceanography 24, PA4216. http://dx.doi.org/10.1029/2008PA001683.

DePaolo, D.J., 2011. Surface kinetic model for isotopic and trace element fractionation during precipitation of calcite from aqueous solutions. Geochim. Cosmochim. Acta 75, 1039–1056. http://dx.doi.org/10.1016/j.gca.2010.11.020.

Fantle, M.S., DePaolo, D.J., 2007. Ca isotopes in carbonate sediment and pore fluid from ODP Site 807A: The Ca^{2+}(aq)–calcite equilibrium fractionation factor and calcite recrystallization rates in Pleistocene sediments. Geochim. Cosmochim. Acta 71, 2524–2546. http://dx.doi.org/10.1016/j.gca.2007.03.006.

Fantle, M.S., Higgins, J., 2014. The effects of diagenesis and dolomitization on Ca and Mg isotopes in marine platform carbonates: implications for the geochemical cycles of Ca and Mg. Geochim. Cosmochim. Acta 142, 458–481. http://dx.doi.org/10.1016/j.gca.2014.07.025.

Flower, B.P., Kennett, J.P., 1994. The middle Miocene climatic transition: East Antarctic ice sheet development, deep ocean circulation and global carbon cycling. Palaeogeogr. Palaeoclimatol. Palaeoecol. 108, 537–555. http://dx.doi.org/10.1016/0031-0182(94)90251-8.

Friedman, I., Murata, K.J., 1979. Origin of dolomite in Miocene Monterey Shale and related formations in the Temblor Range, California. Geochim. Cosmochim. Acta 43, 1357–1365. http://dx.doi.org/10.1016/0016-7037(79)90126-1.

Galy, A., Belshaw, N.S., Halicz, L., O'Nions, R.K., 2001. High-precision measurement of magnesium isotopes by multiple-collector inductively coupled plasma mass spectrometry. Int. J. Mass Spectrom. 208, 89–98. http://dx.doi.org/10.1016/S1387-3806(01)00380-3.

Galy, A., Yoffe, O., Janney, P.E., Williams, R.W., Cloquet, C., Alard, O., Halicz, L., Wadhwa, M., Hutcheon, I.D., Ramon, E., Carignan, J., 2003. Magnesium isotope heterogeneity of the isotopic standard SRM980 and new reference materials for magnesium-isotope-ratio measurements. J. Anal. At. Spectrom. 18, 1352–1356. http://dx.doi.org/10.1039/B309273A.

Hennessy, J., Knauth, L.P., 1985. Isotopic variations in dolomite concretions from the Monterey Formation, California. J. Sediment. Petrol. 55, 120–130. http://dx.doi.org/10.1306/212F862F-2B24-11D7-8648000102C1865D.

Hesse, R., Harrison, W.E., 1981. Gas hydrates (clathrates) causing pore-water freshening and oxygen isotope fractionation in deep-water sedimentary sections of terrigenous continental margins. Earth Planet. Sci. Lett. 55, 453–462. http://dx.doi.org/10.1016/0012-821X(81)90172-2.

Heuser, A., Eisenhauer, A., 2008. The calcium isotope composition ($\delta^{44/40}$Ca) of NIST SRM 915b and NIST SRM 1486. Geostand. Geoanal. Res. 32, 311–315. http://dx.doi.org/10.1111/j.1751-908X.2008.00877.x.

Higgins, J.A., Fischer, W.W., Schrag, D.P., 2009. Oxygenation of the ocean and sediments: consequences for the seafloor carbonate factory. Earth Planet. Sci. Lett. 284, 25–33. http://dx.doi.org/10.1016/j.epsl.2009.03.039.

Higgins, J.A., Schrag, D.P., 2010. Constraining magnesium cycling in marine sediments using magnesium isotopes. Geochim. Cosmochim. Acta 74, 5039–5053. http://dx.doi.org/10.1016/j.gca.2010.05.019.

Holmden, C., 2009. Ca isotope study of Ordovician dolomite, limestone, and anhydrite in the Williston Basin: implications for subsurface dolomitization and local Ca cycling. Chem. Geol. 268, 180–188. http://dx.doi.org/10.1016/j.chemgeo.2009.08.009.

Isaacs, C.M., Petersen, N.F., 1987. Petroleum in the Miocene Monterey Formation, California. Van Nostrand-Reinhold, pp. 83–116.

Jacobson, A.D., Holmden, C., 2008. δ^{44}Ca evolution in a carbonate aquifer and its bearing on the equilibrium isotope fractionation factor for calcite. Earth Planet. Sci. Lett. 270, 349–353. http://dx.doi.org/10.1016/j.epsl.2008.03.039.

Komiya, T., Suga, A., Ohno, T., Han, J., Guo, J., Yamamoto, S., Hirata, T., Li, Y., 2008. Ca isotopic compositions of dolomite, phosphorite and the oldest animal embryo fossils from the Neoproterozoic in Weng'an, South China. Gondwana Res. 14, 209–218. http://dx.doi.org/10.1016/j.gr.2007.10.004.

Kozdon, R., Eisenhauer, A., Weinelt, M., Meland, M.Y., Nürnberg, D., 2009. Reassessing Mg/Ca temperature calibrations of *Neogloboquadrina pachyderma* (sinistral) using paired $\delta^{44/40}$Ca and Mg/Ca measurements. Geochem. Geophys. Geosyst. 10, Q03005. http://dx.doi.org/10.1029/2008GC002169.

Lawrence, J.R., Gieskes, J.M., Broecker, W.S., 1975. Oxygen isotope and cation composition of DSDP pore waters and the alteration of Layer II basalts. Earth Planet. Sci. Lett. 27, 1–10. http://dx.doi.org/10.1016/0012-821X(75)90154-5.

Loyd, S.J., Corsetti, F.A., Eiler, J.M., Tripati, A.K., 2012. Determining the diagenetic conditions of concretion formation: assessing temperatures and pore waters using clumped isotopes. J. Sediment. Res. 82, 1006–1016. http://dx.doi.org/10.2110/jsr.2012.85.

Malone, M.J., Baker, P.A., Burns, S.J., 1994. Recrystallization of dolomite: evidence from the Monterey Formation (Miocene), California. Sedimentology 41, 1223–1239. http://dx.doi.org/10.1111/j.1365-3091.1994.tb01450.x.

Malone, M.J., Claypool, G., Martin, J.B., Dickens, G.R., 2002. Variable methane fluxes in shallow marine systems over geologic time: the composition and origin of pore waters and authigenic carbonates on the New Jersey shelf. Mar. Geol. 189, 175–196. http://dx.doi.org/10.1016/S0025-3227(02)00474-7.

Mazzullo, S.J., 2000. Organogenic dolomitization in peritidal to deep-sea sediments. J. Sediment. Res. 70, 10–23. http://dx.doi.org/10.1306/2DC408F9-0E47-11D7-8643000102C1865D.

Miller, N., Leybourne, M., 2003. Reconstructing basin bottom-water evolution from microbial time capsules: rare earth element geochemistry of organogenic dolomite in the Miocene Monterey Formation. Geological Society of America Abstracts, Seattle, Washington, USA, p. 597.

Miller, N.R., 1995. Lithostratigraphic signal evaluation of the Miocene Monterey Formation, South Elwood Field, Santa Barbara-Ventura Basin, California. Ph.D. thesis. University of Texas at Dallas.

Miller, N.R., Leybourne, M.I., 2010. Anoxic deep-sea microbial dolomite as a paleoceanographic archive – new insights from old "bugs". In: AGU Fall Meeting Abstracts. San Francisco, California, USA, pp. PP11A–1426.

Mozley, P.S., Burns, S.J., 1993. Oxygen and carbon isotopic composition of marine carbonate concretions: an overview. J. Sediment. Petrol. 63, 73–83. http://dx.doi.org/10.1306/D4267A91-2B26-11D7-8648000102C1865D.

Orr, W.L., 1986. Kerogen/asphaltene/sulfur relationships in sulfur-rich Monterey oils. Org. Geochem. 10, 499–516. http://dx.doi.org/10.1016/0146-6380(86)90049-5.

Pisciotto, K.A., Garrison, R.E., 1981. Lithofacies and Depositional Environments of the Monterey Formation, California. Society of Economic Paleontologists and Mineralogists, pp. 97–122.

Pisciotto, K.A., Mahoney, J.J., 1981. Isotopic survey of diagenetic carbonates, Deep Sea Drilling Project Leg 63. In: Initial Reports of the Deep Sea Drilling Project, vol. 63, pp. 595–609.

Pogge von Strandmann, P.A.E., 2008. Precise magnesium isotope measurements in core top planktic and benthic foraminifera. Geochem. Geophys. Geosyst. 9, Q12015. http://dx.doi.org/10.1029/2008GC002209.

Richter, F.M., DePaolo, D.J., 1987. Numerical models for diagenesis and the Neogene Sr isotopic evolution of seawater from DSDP Site 590B. Earth Planet. Sci. Lett. 83, 27–38. http://dx.doi.org/10.1016/0012-821X(87)90048-3.

Richter, F.M., Mendybaev, R.A., Christensen, J.N., Hutcheon, I.D., Williams, R.W., Sturchio, N.C., Beloso Jr., A.D., 2006. Kinetic isotopic fractionation during diffusion of ionic species in water. Geochim. Cosmochim. Acta 70, 277–289. http://dx.doi.org/10.1016/j.gca.2005.09.016.

Sass, E., Bein, A., Almogi-Labin, A., 1991. Oxygen-isotope composition of diagenetic calcite in organic-rich rocks: evidence for δ^{18}O depletion in marine anaerobic pore water. Geology 19, 839–842. http://dx.doi.org/10.1130/0091-7613(1991)019<0839:OICODC>2.3.CO;2.

Schrag, D.P., Higgins, J.A., Macdonald, F.A., Johnston, D.T., 2013. Authigenic carbonate and the history of the global carbon cycle. Science 339, 540–543. http://dx.doi.org/10.1126/science.1229578.

Sun, X., Turchyn, A.V., 2014. Significant contribution of authigenic carbonate to marine carbon burial. Nat. Geosci. 7, 201–204. http://dx.doi.org/10.1038/NGEO2070.

Tipper, E.T., Galy, A., Bickle, M.J., 2008. Calcium and magnesium isotope systematics in rivers draining the Himalaya–Tibetan–Plateau region: lithological or fractionation control? Geochim. Cosmochim. Acta 72, 1057–1075. http://dx.doi.org/10.1016/j.gca.2007.11.029.

Turchyn, A.V., DePaolo, D.J., 2011. Calcium isotope evidence for suppression of carbonate dissolution in carbonate-bearing organic-rich sediments. Geochim. Cosmochim. Acta 75, 7081–7098. http://dx.doi.org/10.1016/j.gca.2011.09.014.

Vasconcelos, C., McKenzie, J.A., Bernasconi, S., Grujic, D., Tien, A.J., 1995. Microbial mediation as a possible mechanism for natural dolomite formation at low temperatures. Nature 377, 220–222. http://dx.doi.org/10.1038/377220a0.

Vasconcelos, C., McKenzie, J.A., Warthmann, R., Bernasconi, S.M., 2005. Calibration of the δ^{18}O paleothermometer for dolomite precipitated in microbial cultures and natural environments. Geology 33, 317–320. http://dx.doi.org/10.1130/G20992.1.

Videtich, P.E., 1981. A method for analyzing dolomite for stable isotopic composition. J. Sediment. Res. 51, 661–662. http://dx.doi.org/10.1306/212F7D38-2B24-11D7-8648000102C1865D.

Wimpenny, J., Colla, C.A., Yin, Q.Z., Rustad, J.R., Casey, W.H., 2014. Investigating the behaviour of Mg isotopes during the formation of clay minerals. Geochim. Cosmochim. Acta 128, 178–194. http://dx.doi.org/10.1016/j.gca.2013.12.012.

Wombacher, F., Eisenhauer, A., Böhm, F., Gussone, N., Regenberg, M., Dullo, W.C., Rüggeberg, A., 2011. Magnesium stable isotope fractionation in marine biogenic calcite and aragonite. Geochim. Cosmochim. Acta 75, 5797–5818. http://dx.doi.org/10.1016/j.gca.2011.07.017.

Yeats, R.S., Haq, B.U., 1981. In: Site 467: San Miguel gap. In: Initial Reports of the Deep Sea Drilling Project, vol. 63, pp. 23–112.